Investigations on the spin-glass state in $Dy_{0.5}Sr_{0.5}MnO_3$ single crystals through structural, magnetic and thermal properties

2008 J. Phys.: Condens. Matter 20 275234

(http://iopscience.iop.org/0953-8984/20/27/275234)

J. Phys.: Condens. Matter **20** (2008) 275234 (10pp) doi:10.1088/0953-8984/20/27/275234

Investigations on the spin-glass state in $Dy_{0.5}Sr_{0.5}MnO_3$ single crystals through structural, magnetic and thermal properties

S Harikrishnan[1], C M Naveen Kumar[1], H L Bhat[1], Suja Elizabeth[1], U K Rößler[2], K Dörr[2], S Rößler[3] and S Wirth[3]

[1] Department of Physics, Indian Institute of Science, C V Raman Avenue, Bangalore 560012, India
[2] IFW Dresden, Postfach 270016, D-01171 Dresden, Germany
[3] Max Planck Institute for Chemical Physics of Solids, Nöthnitzer Straße 40, D-01187 Dresden, Germany

E-mail: liz@physics.iisc.ernet.in

Received 14 February 2008, in final form 5 May 2008
Published 6 June 2008
Online at stacks.iop.org/JPhysCM/20/275234

Abstract

Single crystals of $Dy_{0.5}Sr_{0.5}MnO_3$ are grown using the optical floating zone technique, and their structural, magnetic, transport and thermal properties have been investigated. Magnetization measurements under field-cooled and zero-field-cooled conditions display irreversibility below 35 K. The magnetization does not saturate up to fields of 5 T in the temperature range 5–350 K. AC susceptibility shows a cusp around 32 K that shifts to higher temperature with increasing frequency. This frequency dependence of the peak temperature follows a critical slowing down with exponent $z\nu = 3.6$. Electrical resistivity shows insulating behavior, and the application of magnetic fields up to 10 T does not change this qualitative behavior. However, a marked negative magnetoresistance is observed in the paramagnetic phase reaching 80% at 70 K and 10 T. The observed resistivity behavior does not obey an activated type of conduction. These features are characteristic of spin-glass behavior in this half-doped insulating manganite. It is argued that the spin-glass-like state originates from the A-site disorder, which in turn results from the random distribution of cations with different ionic radii. Specific-heat measurements reveal a sizable linear contribution at low temperature that may be associated with the glassy magnetic ordering and a Schottky-like anomaly in a wide temperature range between 8 and 40 K. The distribution of Schottky levels is explained by the inhomogeneity of the molecular field in the spin-glass state that leads to variable splitting of the Kramers ground-state doublets in Dy^{3+}.

(Some figures in this article are in colour only in the electronic version)

1. Introduction

Many investigations on $(RE)_{1-x}A_xMnO_3$ (RE = rare earth ion, A = alkaline earth ion) have focused on how the transport and magnetic properties are influenced by the cation size and the disorder effect at the A-site [1–3]. Substitution of cations with different ionic radii at the A-site distorts the structure, introduces disorder and enhances antiferromagnetic superexchange interactions over ferromagnetic interactions. Raveau *et al* [4] found size mismatch and A-site cationic disorder to be detrimental to the colossal magnetoresistive (CMR) properties of ferromagnetic manganites near ideal doping and a crucial factor for generating a spin-glass insulating state. Moreover, global phase diagrams of manganites suggest a

systematic relation of their magnetic and electrical properties with the one-electron bandwidth and the quenched disorder through the mixed occupation on the A-site. These phase diagrams can be presented in dependence on the average A-site radius $\langle r_A \rangle$ and its variance σ [5]. Here, the variance introduced by Rodriguez-Martinez and Attfield [6]:

$$\sigma^2 = \Sigma_i y_i r_i^2 - \langle r_A \rangle^2,$$

quantifies the disorder due to the random distribution of cations at the A-site, where y_i is the fractional occupancy of the A-site by the ith ion type and r_i are the corresponding ionic radii. Akahoshi *et al* [7] found that the intrinsic disorder in A-site disordered $Ln_{0.5}Ba_{0.5}MnO_3$ enhances fluctuations between ferromagnetic and antiferromagnetic interactions and can result in a magnetic glassy state, different from the behavior of A-site ordered compounds. Manganites with low σ^2 usually show ferromagnetic metallic nature (FMM) in their ground state. In a series of manganites near 50:50 doping for one type of divalent A-atom, substitution of different R-atoms changes both σ^2 and $\langle r_A \rangle$ [8, 5]. As σ^2 increases in such a series, a charge ordered antiferromagnetic (CO-AFM) state is usually stabilized and further increases in σ^2 lead to a spin-glass insulating state [9]. It is found that magnetic long-range order is stable for $\sigma^2 = 10^{-3}$ Å^2, whereas a magnetic glassy state dominates above $\sigma^2 \approx 10^{-2}$ Å^2. With $\sigma^2 = 0.003$ Å^2 for $Nd_{0.55}(Ca_{0.45}Sr_{0.55})_{0.45}MnO_3$, the system exhibits a metal–insulator transition typical for the CMR behavior. At an intermediate value of $\sigma^2 = 0.008$ Å^2 (e.g. $Nd_{0.55}(Ca_{0.76}Ba_{0.24})_{0.45}MnO_3$), a charge ordered antiferromagnetic state is observed [10]. Eventually, for $\sigma^2 = 10^{-2}$ Å^2 (e.g. $Gd_{0.55}Sr_{0.45}MnO_3$ with $\sigma^2 = 0.009$) spin-glass properties emerge and a system like $Sm_{0.55}(Ca_{0.6}Ba_{0.4})_{0.45}MnO_3$ ($\sigma^2 = 0.015$) shows a glassy state with $T_f \approx 42$ K [10]. Compared to σ^2, an opposite trend is observed in the dependence on the average radius $\langle r_A \rangle$. When the average radius is large, the FMM state is stable [1] and, hence, manganites with large $\langle r_A \rangle$ do not show spin-glass behavior. Consequently, $La_{0.7}Ca_{0.3}MnO_3$ with $\langle r_A \rangle = 1.244$ Å exhibits a ferromagnetic metallic nature. If $\langle r_A \rangle$ decreases, the FMM state transforms into the CO-AFM one on cooling, as observed in $Nd_{0.5}Sr_{0.5}MnO_3$ with $\langle r_A \rangle = 1.236$ Å [11]. Further decrease in $\langle r_A \rangle$ usually causes an insulating spin-glass-like magnetic state [12] and the Mn–O–Mn bond angle deviates more from 180°. This results in a reduced one-electron bandwidth which, in turn, leads to an antiferromagnetic insulating state. In agreement with this general trend are the examples $Gd_{0.55}Sr_{0.45}MnO_3$ ($\langle r_A \rangle = 1.20$ Å), which exhibit spin-glass properties [13], and $Y_{0.5}Ca_{0.5}MnO_3$ with $\langle r_A \rangle = 1.13$ Å that show no ferromagnetism, instead signatures of a spin-glass state are found [14].

At present, it is not understood why the spin-glass ordering temperature in such systems is so strongly reduced compared with the transition temperatures that establish the competing long-range CO-AFM or FM states in rather similar manganites. Because of the dense Mn sublattice one possibly cannot classify the mixed-valent manganites as the usual spin-glass materials like the classical dilute metallic alloys [15]. Magnetic glassy behavior in these systems poses an interesting problem. Because of their complex phase diagrams with competing phases, many manganites are possibly close to first-order magnetic phase transitions. In particular, half-doped systems $RE_{0.5}A_{0.5}MnO_3$ can display transitions from FM to CO-AFM phases. Owing to the intrinsic randomness in these mixed compounds, the bicritical features of phase coexistence can be smeared out and can lead to various mesoscopic or microscopic heterogeneities [5]. On the other hand, the competition between ferromagnetic double-exchange and antiferromagnetic superexchange naturally leads to frustrated magnetic couplings in the manner of a $\pm J$ exchange model, if the microscopic disorder allows for the simultaneous occurrence of both types of couplings in the Mn–O sublattice. The two mechanisms could lead to either a mixed FM and CO-AFM domain state with glassy or superparamagnetic properties, or to a homogeneous spin-glass state. The distinction between these two possibilities would contribute to our understanding of the phase structure of the manganites.

For the series of half-doped manganites with A = Sr, Pr, Nd evidence for CO-AFM and the competition with FM was found [16, 11]. For the complete series and, in particular, for RE with smaller radii, only a few properties have been reported, including spin-glass states for RE = Eu, Gd, Tb, Dy and Y [17–19]. For the Y-based system, rather conventional spin-glass properties were found by detailed magnetic measurements [20]. For the Nd- and Ho-based systems, structural inhomogeneity with a coexistence of different crystal structures on a scale of several tens of nm have been reported and were ascribed to compositional fluctuations [21–23]. Structural inhomogeneities, along with small regions with A-type CO-AFM, were observed in $Ho_{0.5}Sr_{0.5}MnO_3$ by Autret *et al* [23]. These inhomogeneities could underlie the magnetically glassy or superparamagnetic properties in this system, which is very similar to the little investigated $Dy_{0.5}Sr_{0.5}MnO_3$. Therefore, $Dy_{1-x}Sr_xMnO_3$ is an interesting candidate for investigations on the spin-glass state in the half-doped mixed-valent manganites at low temperature. $Dy_{0.5}Sr_{0.5}MnO_3$ has a $\langle r_A \rangle$ value of 1.19 Å and a σ^2 value of 0.0129 Å^2. Thus, both criteria for a spin-glass behavior due to the size and quenched disorder of the A-site ions are fulfilled. Moreover, the Dy ions may magnetically couple to the magnetic order of the Mn–O subsystem, which allows us to use the 4f magnetism of the rare earth as a probe of the magnetic states in this system. Here, we report and analyze basic physical properties of $Dy_{0.5}Sr_{0.5}MnO_3$ single crystals.

2. Experimental details

Single crystals of $Dy_{0.5}Sr_{0.5}MnO_3$ were grown by the optical floating zone method in an IR image furnace (FZ-T-10000-H-VI-VP procured from Crystal Systems Inc). The x-ray powder diffraction (XRD) pattern was measured for ground powder from a piece of such a crystal using a Philips X'pert diffractometer with Cu Kα radiation. The

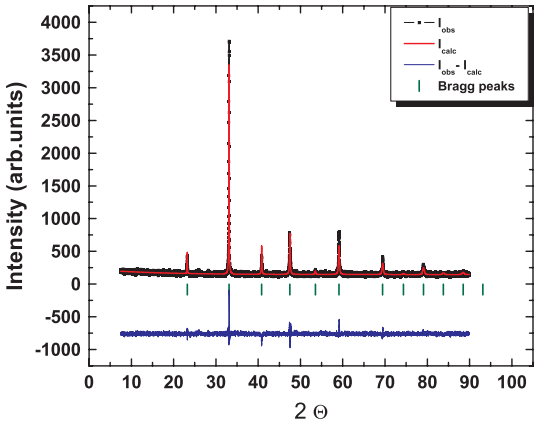

Figure 1. X-ray diffraction pattern of powdered $Dy_{0.5}Sr_{0.5}MnO_3$ at room temperature using Cu Kα radiation, and Rietveld refinement including fit and difference. The series of tick marks allowed Bragg reflections. (Quality measures of refinement: $R_p = 4.71$, $R_{wp} = 6.57$, $R_{exp} = 3.90$, $\chi^2 = 2.85$.)

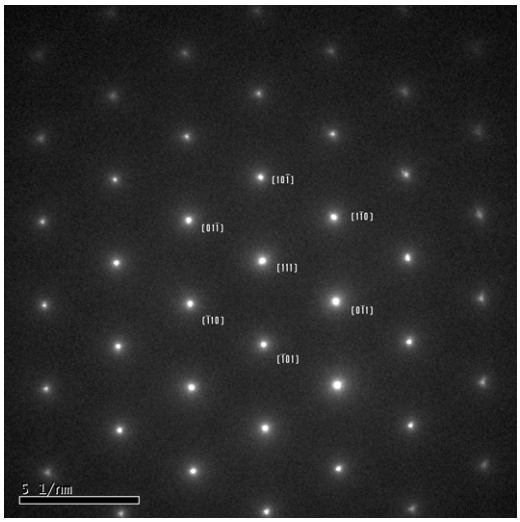

Figure 2. Selected-area diffraction (SAD) pattern obtained through TEM.

diffraction pattern was refined with the Rietveld method [24] by using the FULLPROF [25] code. Selected-area diffraction (SAD) images from the single crystals were obtained from transmission electron microscopy using a Tecnai G 30, 300 kV spectrometer. Magnetic measurements were conducted in a superconducting quantum interference device (SQUID) magnetometer. DC magnetization in the field-cooled (FC) and zero-field-cooled (ZFC) cycles were measured at different applied fields of 0.002, 0.01 and 0.3 T. The magnetization isotherms at different temperatures (5–350 K) were also recorded. AC susceptibility and specific-heat (zero-field) measurements were performed in a commercial physical properties measuring system (PPMS Quantum Design). Electrical resistivity was measured by the standard four-probe method.

3. Results

3.1. Crystal structure

The crystal structure of $Dy_{0.5}Sr_{0.5}MnO_3$ has been refined in the pseudo-cubic perovskite structure with space group $Pm3m$. The observed, calculated and difference patterns after the refinement are shown in figure 1. Absence of any superstructure peaks in the XRD pattern indicates a homogeneous mixed-valence state. The lattice parameter obtained is 3.825 Å which is close to the ideal undistorted cubic structure. This is remarkable as the small A-site radius $\langle r_A \rangle$ indicates a distorted perovskite structure by the small tolerance factor $t = [\langle r_A \rangle + r_O]/\sqrt{(2)}[\langle r_{Mn} \rangle + r_O] \simeq 0.919$ for $Dy_{0.5}Sr_{0.5}MnO_3$. However, owing to the large A-site disorder σ^2, the lattice structure is likely to be inhomogeneously distorted on the scale of unit cells. These effects possibly cannot be observed by low-resolution diffraction, and the XRD pattern only displays an average nearly ideal cubic perovskite lattice. The unit cell volume calculated from the refined cell parameters is 55.95 $Å^3$. The determined lattice parameter and unit cell volume are close to the 3.824 and 55.92 $Å^3$ obtained by Kasper *et al* for polycrystalline $Dy_{0.5}Sr_{0.5}MnO_{3-\gamma}$ with a small oxygen deficiency $\gamma \simeq 0.06$ [18]. Interestingly, the unit cell volume is not very different from the value for $Nd_{0.5}Sr_{0.5}MnO_3$ (56.69 $Å^3$) despite the large difference in ionic radii of the A-site cation (Nd = 1.16 Å and Dy = 1.08 Å). A selected-area electron diffraction pattern of $Dy_{0.5}Sr_{0.5}MnO_3$ is shown in figure 2. The pattern is indexed along the [1 1 1] cubic zone axis. There is no evidence of superlattice spots from any long-range structural order in the system at room temperature. Thus, the SAD pattern also supports the structure solution from the XRD data.

3.2. Magnetization

Magnetization M versus temperature curves for $Dy_{0.5}Sr_{0.5}MnO_3$ show a clear bifurcation in the ZFC and FC cycles at low applied magnetic fields $\mu_0 H = 0.002$ T (figure 3(a)). The splitting happens at $T_{irr} \simeq 35$ K. At higher applied fields of 0.01 T the bifurcation between the ZFC and FC cycles appears to be smeared out over a larger temperature interval. No sign of saturation is observed, possibly due to the large paramagnetic susceptibility of Dy that masks the magnetic anomaly (figure 3(a)). Therefore, the thermal magnetization data indicate the onset of glassy magnetic properties around 35 K. The inverse susceptibility above 100 K, as derived from the magnetization data with an applied field of 0.002 T, was fitted to a Curie–Weiss law (figure 3(b)). The effective paramagnetic moment calculated from the fit, $\mu_{eff} = 10.90\ \mu_B$, is close to the ideal value of 10.6 μ_B calculated assuming contributions only from the spin moments of Mn^{3+}/Mn^{4+} and the spin and orbital contributions from the Dy^{3+} ion. The Weiss temperature, θ_W, from the fit is −61.5 K, indicating rather strong antiferromagnetic interactions. Isothermal magnetization curves in the temperature range 5–350 K are presented in figure 4(a). As can be seen from the figure, the magnetization does not saturate even at an applied field of 5 T over the whole temperature range, thus effectively ruling out long-range ferromagnetic order. However, at 5 K a small but clear hysteresis is seen. M versus

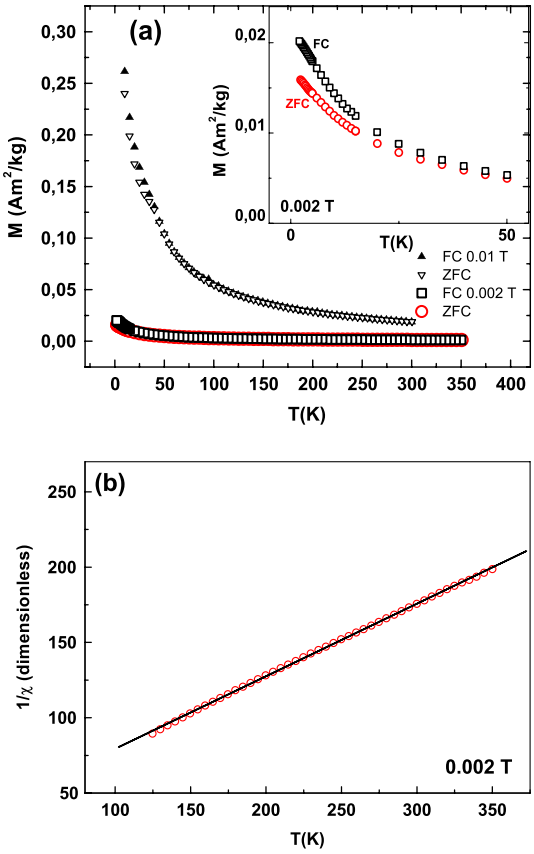

Figure 3. (a) Zero-field-cooled (ZFC) and field-cooled (FC) magnetization at applied fields of 0.002 T and 0.1 T, respectively. The inset magnifies the splitting between ZFC and FC magnetization for 0.002 T. (b) Curie–Weiss fit in the paramagnetic temperature range down to 100 K.

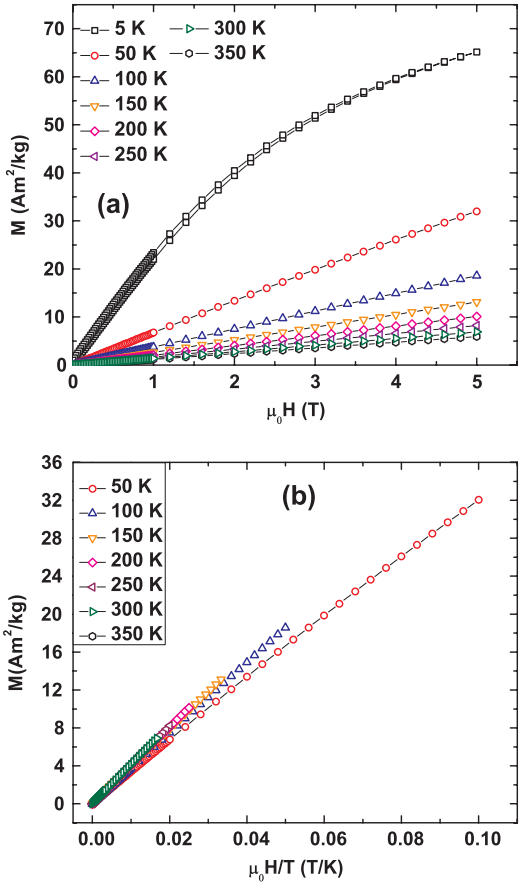

Figure 4. (a) Magnetization isotherms at different temperatures 5–350 K. At 5 K a small hysteresis is observed. (b) M versus H/T plots indicates that the scaling fails below 150 K.

H/T plots (figure 4(b)) obtained from the magnetization isotherms show that H/T scaling of magnetization is violated below ∼150 K. Thus, static magnetization data rule out a superparamagnetic behavior due to a distribution of independent magnetic clusters [27], see also section 2.10 in [15]. This will be confirmed below by dynamic magnetization measurements.

3.3. AC susceptibility

The real part of the ac susceptibility χ' of $Dy_{0.5}Sr_{0.5}MnO_3$ in the frequency range 10–10 000 Hz is presented in figure 5(a). The inset of figure 5(a) shows the imaginary part of the susceptibility χ'' at 10 kHz. This χ'' exhibits a peak at about 35 K, decreases towards lower temperature, experiences a minimum at about 4 K and then increases again. The peak at 35 K is due to the onset of glassy dynamics, whereas the increase of the susceptibility below 4 K is probably related to magnetic ordering of the Dy moments. Above this low temperature region, where ordering effects of the Dy sublattice are expected, a strong overall contribution from the large paramagnetic Dy moments is found. This accounts for the major part of the increasing in-phase susceptibility χ' with decreasing temperature. The peak in the real part of the susceptibility $\chi'(T)$ around 33–36 K shifts to higher temperature at higher applied frequencies. For a proper spin-glass transition one expects that dynamical scaling holds near a critical temperature T_c, which corresponds to the ideal static spin-glass transition. Hence, the susceptibility should obey critical scaling [15]. The apparent spin-glass temperatures $T_{sg}(f)$ at finite frequency f as fixed by the temperatures at the peak of the $\chi'(T)$ data should be described by a power law near the critical temperature T_c:

$$T_{sg}(f) = T_c\,(1 + (\tau_0 f)^{1/z\nu}), \tag{1}$$

where $z\nu$ are critical exponents and τ_0 is a microscopic timescale. In order to analyze the dynamical scaling near the spin-glass transition temperature, the peak temperatures in the real part of the ac susceptibility curves had to be determined accurately. First, a background contribution for the paramagnetic Dy was determined from the raw data for $\chi'(T)$ for the highest driving frequency $f = 10$ kHz by fitting the Curie–Weiss law in the combined range of $T < 20$ K and $T > 60$ K excluding the temperature range of the spin-glass transition. The peak around the transition for all studied frequencies was obtained by subtracting this background. The difference plots are shown in figure 5(b). The anomalies around 32–35 K are now discernible as cusps, which is typical for spin-glass ordering. Another low temperature peak is located below 10 K. It corresponds to an increase of

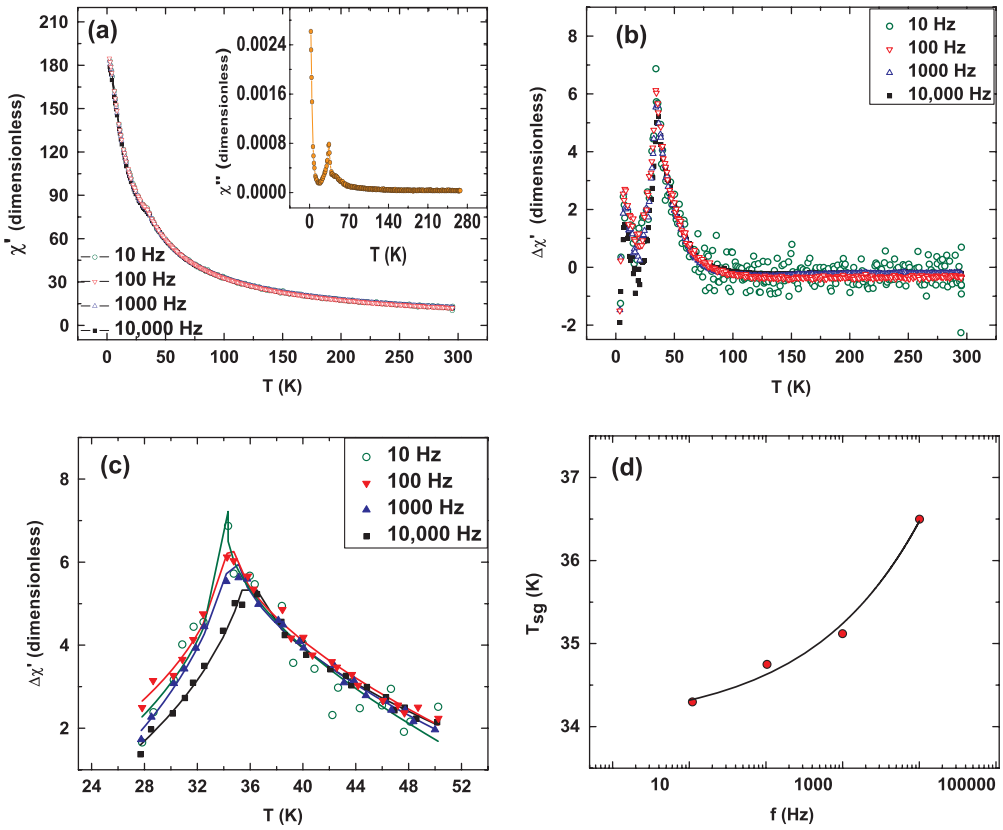

Figure 5. (a) AC susceptibility for frequencies from 10 to 10,000 Hz. A cusp is seen at around 35 K. (b) Anomaly $\Delta\chi'(T)$ obtained by subtracting a paramagnetic background contribution. (c) Cusps of $\Delta\chi'(T)$ and fits for determination of the apparent frequency-dependent spin-glass temperatures $T_{sg}(f)$ near the spin-glass transition. (d) Power-law fit $T_{sg}(f)$ according to equation (1).

the loss part χ'' towards low temperatures. This indicates another magnetic transition possibly related to a sluggish magnetic ordering of the Dy moments. The frequency-dependent apparent spin-glass transition temperatures $T_{sg}(f)$ were obtained by fitting the difference data for each frequency in figure 5(b) by two branches of power laws with positive exponents and a common constant background, $T_{sg} = a(T - T_{sg})^{\alpha} + c$ and $T_{sg} = b(T_{sg} - T)^{\beta} + c$, above and below T_{sg}, respectively. From the peak temperatures $T_{sg}(f)$ the critical exponent governing the spin-glass relaxation can be estimated from a fit to the power-law equation (1). This fit is shown in figure 5(d). From this fit, the critical spin-glass temperature $T_c = 33.9(2)$ K, the critical exponent $z\nu = 3.6(7)$ and the microscopic characteristic spin-flip time $\tau_0 \simeq 1.0(9) \times 10^{-8}$ s can be determined.

In view of the relatively large uncertainties in this fit, other possibilities to explain the glassy magnetic behavior must be taken into account. A peak in the susceptibility versus temperature usually signifies either a glassy or a superparamagnetic state. In order to distinguish between these two possibilities the relative change of the apparent spin-glass transition temperature T_{sg} with frequency on a logarithmic scale:

$$K = \frac{\Delta T_{sg}}{T_{sg}\Delta \log(f)},$$

can be calculated [15]. Here, Δ refers to the difference between measurements at different frequencies. For a spin-glass system K is of the order of 0.01, and for superparamagnets K is expected to be greater than 0.1 [15]. For $Dy_{0.5}Sr_{0.5}MnO_3$, K has a value of 0.0135. Moreover a fit to the thermally activated Arrhenius behavior

$$f = f_0 \exp(-E_b/k_B T_{sg})$$

yields unrealistically high values for the characteristic attempt frequency $f_0 = 2.28 \times 10^{28}$ Hz and for the barrier height $E_b/k_B = 825$ K. This failure of the Arrhenius model again rules out superparamagnetism [15].

3.4. Resistivity

The measured electrical resistivity of $Dy_{0.5}Sr_{0.5}MnO_3$ is presented in figure 6(a), indicating an insulating or semiconducting behavior with a steep rise on cooling, similar to other manganite spin-glass systems [26, 28]. The data are restricted to the paramagnetic state for higher temperatures above the spin-glass transition, because on approaching T_c, the rise of resistivity in $Dy_{0.5}Sr_{0.5}MnO_3$ is so steep that no measurement was possible anymore below 50 K. Moreover, application of a 10 T magnetic field does not significantly change this qualitative behavior of the resistivity. Still, the magnetoresistance, calculated as $MR = (\rho(H) - \rho(0))/\rho(0)$, gradually increases towards low temperatures and reaches large values, as shown for an applied field of $\mu_0 H = 10$ T in the inset of figure 6(a).

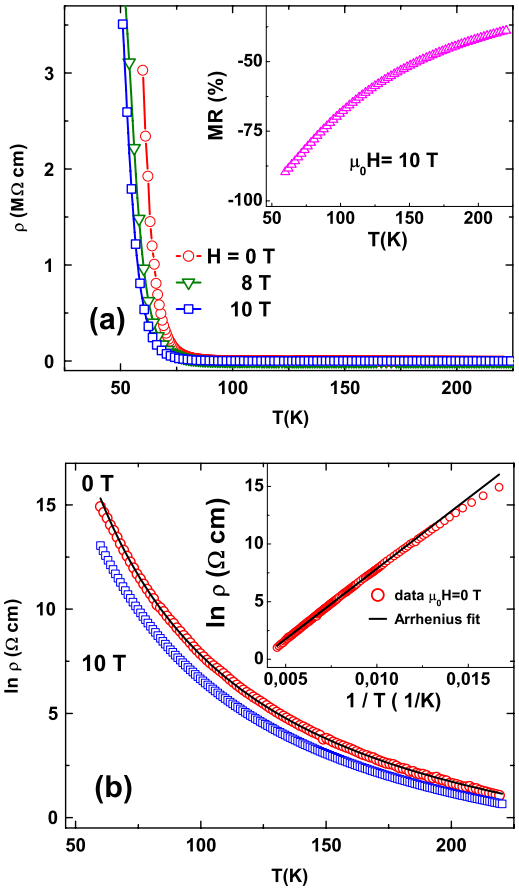

Figure 6. (a) Electrical resistivity of $Dy_{0.5}Sr_{0.5}MnO_3$ indicates an insulating behavior. Magnetoresistance $MR(T)$ at a field of 10 T is shown in the inset. (b) Plot of $\ln \rho$ versus T with a fit for zero-field data in the form of variable-range-hopping equation (2). The inset shows the same data in an Arrhenius plot with a corresponding fit for the high temperature range.

Hence, the resistivity is strongly influenced by magnetic scattering of charge carriers in the paramagnetic state. At 50 K above the spin-glass temperature, the material becomes so strongly insulating that measurements of resistivity through the magnetic anomaly were impossible. Figure 6(b) presents the plot of $\ln \rho$ versus T and shows a fit of the zero-field data to the expression

$$\rho(T) = \rho_0 \exp\left[(T_0/T)^{\kappa}\right] \qquad (2)$$

appropriate for variable-range-hopping (VRH) type conduction with a characteristic temperature T_0 and an exponent κ. From the fit, we find $T_0 = 3.02(9) \times 10^3$ K and the exponent $\kappa = 0.79(1)$. The inset shows the fit of high temperature data to the Arrhenius relation:

$$\rho = \rho_0 \exp(E_a/k_B T)$$

and the activation energy E_a estimated as 0.11 eV (equivalent to $E_a/k_B = 1300$ K). This value is comparable to the E_a value observed in similar compounds like $Dy_{0.5}Ca_{0.5}MnO_3$ [29], but the fit is seen to deviate towards low temperature. Therefore, thermally activated transport does not explain the conduction mechanism in this system.

The observed resistivity $\rho(T)$ follows an unconventional behavior, as found above from the fit with the VRH form. The exponent κ should have fixed values, where $\kappa = 1/4$ applies for the Mott regime of uncorrelated hopping carriers and $\kappa = 1/2$ for a system of carriers with a gap due to correlations according to the Efros–Shklovskii mechanism [30, 31]. The found exponent $\kappa \simeq 0.8$ markedly deviates from these values. We have also checked that the observed resistivity versus temperature behavior cannot be explained by theoretical expressions commonly assumed for the paramagnetic semiconducting phases of manganites [32–34]. In particular, small-polaron conductivity, described by $\rho(T)/\rho_0 = T^{\delta} \exp[-E_0/k_B T]$ with exponents $\delta = 1$ or $3/2$ for adiabatic or non-adiabatic hopping, respectively, [35, 33], is not in agreement with our data. An extension of the small-polaron hopping conductivity by using a temperature-dependent activation energy $E_0 = \epsilon_0 + \epsilon/T$, as proposed by Neifeld *et al* [36], also does not yield a valid description of our data. The failure to describe the resistivity behavior by these standard expressions was already noticed earlier in manganites with spin-glass properties, e.g. as a result of Mn-site substitution [37] and due to A-site size-disorder and cluster-glass properties [38]. The expression of the form of the variable-range-hopping equation (2) with different exponents can be justified by a heuristic scaling that takes into account the influence of the static spin disorder on the localization of the charge carriers. This is a mechanism similar to that proposed by Viret *et al* for ferromagnetic manganites [32]. In the Efros–Shklovskii regime, the characteristic temperature depends on the localization length ξ as $T_0 \sim 1/\xi$, while in the Mott regime, one has $T_0 \propto \xi^3$. In a system tending towards disordered spin freezing and with strong spin-dependent scattering of charge carriers, the effective localization length should depend on temperature. Then, the localization length scales with the correlation length L_{sg} of the spin-glass order parameter, $\xi \sim (1/L_{sg})^{\vartheta} \propto 1/|T - T_c|^{\nu\vartheta}$, with an exponent ϑ. The simplest assumption would be an inverse relation between localization length and spin-glass correlations, $\vartheta = 1$. The scaling of resistivity in the Efros–Shklovskii regime should follow as $\rho(T)/\rho_0 \sim \exp[(c/T|T - T_c|^{-\nu\vartheta})^{1/2}] \simeq \exp[(\tilde{T}_0/T)^{1/2-\nu\vartheta/2})]$, where the last approximation for the paramagnetic state holds for $T \gg T_c$. For the Mott regime, one has $\rho(T)/\rho_0 \sim \exp[(c/T|T - T_c|^{3\nu\vartheta})^{1/4}] \simeq \exp[(\hat{T}_0/T)^{1/4+3\nu\vartheta/4}]$. Usual estimates for the exponent of the spin-glass correlation in 3D Ising-like spin-glasses are in the range $\nu = 1.2$–3 [39], and for $Eu_{0.5}Ba_{0.5}MnO_3$ ($\nu = 1.3$) were determined in experiments [40]. Our estimated effective exponent $\kappa \simeq 0.8$ is smaller than the range of values for $1/4 + 3\nu/4 = 1.2$–2.5 for the scaling expression in the Mott regime with $\vartheta = 1$. Hence, a scaling relation between the spin-glass correlations L_{sg} and the electronic localization length with an exponent $\vartheta < 1$ would describe the observed resistivity behavior. For the Efros–Shklovskii regime generally a weaker rise of resistivity with an effective exponent $\kappa < 1/2$ would be found for $\vartheta < \nu$. The scaling expressions suggest that the resistivity can be explained by an anomalous form of variable-range-hopping conductivity due to changing localization length and carrier correlations on the background of a homogeneous spin-glass freezing.

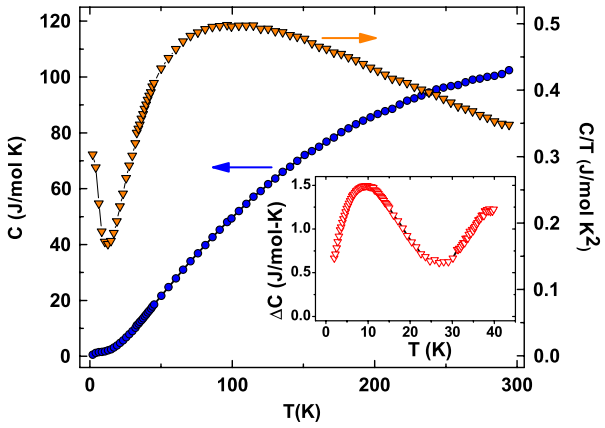

Figure 7. Specific heat of $Dy_{0.5}Sr_{0.5}MnO_3$. The inset shows the excess contribution $\Delta C(T)$ in the low temperature range after subtracting a smooth background.

3.5. Specific heat

The variation of specific heat of $Dy_{0.5}Sr_{0.5}MnO_3$ with temperature is shown in figure 7. A high value of specific heat at lower temperatures is observed in contrast to insulating manganites like $La_{0.8}Ca_{0.2}MnO_3$ [41]. Similar high values of specific heat have been observed in $Dy_{0.5}Ca_{0.5}MnO_3$ studied by Lopez *et al* [42]. Further, a broad shoulder below about 10 K is discernible. In order to get a first rough overview of these anomalies, we have subtracted a suitable background from the measured data for $Dy_{0.5}Sr_{0.5}MnO_3$. As a background, we used specific-heat data for $La_{0.7}Pb_{0.3}MnO_3$ [43]. $La_{0.7}Pb_{0.3}MnO_3$ is a ferromagnetic metallic manganite, which has specific-heat contributions from electronic excitations and spin waves at low temperatures, but it has no anomalies related to rare-earth 4f electrons or glassy magnetic behavior. Therefore, the data for $La_{0.7}Pb_{0.3}MnO_3$ yield a background estimate to the maximum in the low temperature region, which helps to appreciate the magnitude of the anomalies in the specific heat of $Dy_{0.5}Ca_{0.5}MnO_3$. The difference plot in the inset of figure 7 gives qualitative information on the excess contributions $\Delta C(T)$ to the specific heat at low temperature. The main feature is a prominent wide peak below 25 K, which should be associated with a Schottky-like anomaly caused by crystal-field level excitations of 4f electronic states in the Dy ions. The re-increase above 25 K may be related to the spin-glass ordering. However, it is well known that a spin-glass contribution to specific heat rarely shows up as a distinct anomaly in specific heat. More important is the overall high value of $\Delta C(T)$ even after subtracting the specific heat of a similar metallic system. Therefore, we surmise the presence of contributions to the specific heat of the form $S\,T^n$, which may be linear or with a small exponent $n < 2$. These contributions cannot stem from electronic excitations or spin waves in $Dy_{0.5}Sr_{0.5}MnO_3$. A linear specific-heat contribution is expected for glassy magnetic systems [15]. It is quite possible that the dense magnetic system of $Dy_{0.5}Sr_{0.5}MnO_3$ shows this anomaly much more strongly than canonical metallic spin-glasses with dilute magnetic impurities.

The Schottky-like peak in this compound has a long tail that extends up to higher temperatures. A fit assuming only one Schottky level cannot reproduce the observed data in the whole temperature range. To obtain a good fitting model, it was necessary to assume a distribution of Schottky levels. A fit of the low temperature data in the range 2–45 K was performed assuming that the relevant contributions to specific heat arise from the lattice, a magnetic contribution from the spin-glass state and Schottky contribution. The electronic contribution was discarded as the electrical resistivity measurements show that the compound is highly insulating. Thus, the expression for the total specific heat was composed as

$$C_{\rm tot} = C_{\rm latt} + C_{\rm sg} + C_{\rm S} \tag{3a}$$

$$C_{\rm latt} = B_3 T^3 + B_5 T^5 \tag{3b}$$

$$C_{\rm sg} = S T^n \tag{3c}$$

$$C_{\rm S} = \frac{1}{2} R \sum_{i=1}^{N_{\rm S}} w_i \frac{\left(\frac{\Delta_i}{k_{\rm B}T}\right)^2 \exp\left(\frac{\Delta_i}{k_{\rm B}T}\right)}{\left[1+\exp\left(\frac{\Delta_i}{k_{\rm B}T}\right)\right]^2}; \tag{3d}$$

$$\sum_{i=1}^{N_{\rm S}} w_i = 1 \tag{3e}$$

where $C_{\rm latt}$ is the lattice term, $C_{\rm sg}$ is the spin-glass term and $C_{\rm S}$ is the Schottky term (R is the universal gas constant). We assume and later check through fits that the spin-glass contribution is linear in temperature, $n = 1$. The Schottky contribution to the specific heat is described by a discrete distribution of $N_{\rm S}$ two-level systems with different splittings Δ_i and with weight factors w_i. A sequence of parameters for different models according to the definitions in equations (3) is given in table 1. We find that a good overall fit requires at least two ($N_{\rm S} = 2$), or better yet three ($N_{\rm S} = 3$), Schottky levels. Considering the exponent n in $C_{\rm sg}$ as an open fit parameter does not improved the fits as, for example, obvious in the case $N_{\rm S} = 2$ (model IIa). For $N_{\rm S} = 3$ the parameters n, S, B_3 and the energy of the Schottky levels become strongly correlated (a tendency that is even more pronounced for $N_{\rm S} = 4$). The fit results in a redistribution towards low temperatures between the Schottky-like contributions and the spin-glass contribution with an unphysical exponent $n \sim 0.5$. Therefore, model IIIa has to be discarded. On the other hand, omitting the spin-glass contribution $C_{\rm sg}$ does not yield valid fits (see models IIb and IIIb). Hence, an anomalous linear contribution to the specific heat is clearly present in this insulating manganite. We also note that using more than three Schottky levels (model IV with $N_{\rm S} = 4$) does not improve the fit as compared to model III. Based on these findings, we consider model III as the best description of our data. As further support for model III, the residuals of the corresponding fit are presented in figure 8(a) exhibiting no apparent features and being dominated by noise.

The assumed Schottky contributions at least in the lower temperature range $T < 25$ K arise from the split Kramers doublets of the 4f electrons in Dy^{3+} ions. In the model (3*a*) we assumed that the splitting of the ground state is inhomogeneous and that no further crystal-field levels need to be considered. The splittings $\Delta_i/k_{\rm B}$ is proportional to the strength of the local

Table 1. The fitting parameters for models using equation (3*a*) for different numbers of Schottky levels I, II, III and IV. For models with label 'a' the exponent n in C_{sg} was released, while for the models with label 'b' the C_{sg} contribution was omitted by fixing $S \equiv 0$. For the lattice contribution the Debye temperature θ_D is listed. The last column gives the variance of residuals (reduced χ^2) of the fits.

		B_3	θ_D	B_5		S	Δ_i/k_B (K)				χ^2
	N_S	(mJ mol^{-1} K^{-4})	(K)	(10^{-8} J mol^{-1} K^{-6})	n	(J mol^{-1} K$^{-(1+n)}$)	w_i $i = 1, \ldots, N_S$				(10^{-4})
I	1	0.222(14)	352(11)	−4.6(4)	1	0.158(6)	2.11(25)				24.2
							1				
Ia	1	0.222(43)	353(36)	−5(2)	1.00(14)	0.158(6)	2.12(35)				24.5
							1				
II	2	0.288(6)	323(7)	−7.37(24)	1	0.120(3)	7.6(4)	18(2)			6.5
							0.28	0.72			
IIa	2	0.302(11)	318(12)	−7.78(32)	0.89(10)	0.159(48)	7(1)	16(3)			6.1
							0.22	0.78			
IIb	2	0.476(12)	273(6)	−15.1(8)	—	0	11(3)	28(6)			42.4
							0.41	0.59			
III	3	0.256(9)	335(12)	−6.0(2)	1	0.114(7)	6.48(51)	18(1)	106(8)		1.6
							0.27	0.25	0.48		
IIIa	3	0.275(28)	328(34)	−6.1(8)	0.49(12)	0.456(8)	11(6)	23(18)	105(12)		1.2
							0.09	0.07	0.83		
IIIb	3	0.481(28)	272(15)	−15.4(18)	—	0	8(4)	24(4)	106(—)		47.7
							0.28	0.72	—		
IV	4	0.260(16)	334(21)	−6.14(9)	1	0.112(26)	5(9)	10(24)	19(17)	104(24)	1.6
							0.18	0.15	0.22	0.45	

(molecular) field at the Dy sites. The inhomogeneity of the local field at the sites of the Dy can rely on inhomogeneous lattice distortions. However, it must mainly arise due to coupling to the frozen spin-glass state in the Mn–O subsystem. However, the very wide distribution of model III contains a large excitation level $\Delta_3/k_B \simeq 110$ K. Lacking specific information about the crystal-field levels for Dy^{3+} in this type of manganite, it cannot be ruled out that this contribution is, in fact, due to the higher excitation levels of the 4f states. However, the anomaly seen above 25 K in figure 8(b) for the best fitting model may rather be related to the spin-glass ordering or other magnetic effects in this compound. In a homogeneous spin-glass system a sizable fraction of sites experiences a zero local field, which would not contribute to the Zeeman splitting of the ground-state Kramers doublet and would not contribute to the Schottky-like anomaly. In fact, the entropy release calculated from $C_S(T)$ for model III is only about $0.3\,R$ ln 2 at 30 K, i.e. only 60% of the expected full entropy of the Dy Zeeman-split ground-state levels. The lower part of the Schottky-like anomaly still shows an anomalous widening as compared to a single two-level contribution. The 60% of sites contributing to this anomaly represent a realistic fraction of Dy^{3+} sites with strong local fields. In this interpretation, the second anomaly for $T > 30$ K is not necessarily related to the Dy 4f states. Rather, the model only emulates this anomaly possibly related to the spin-glass ordering or a dependent smeared ordering of Dy moments by a distribution of Schottky-like two-level contributions. However, the entropy at higher temperatures above $T > 20$ K is dominated by the linear contribution in the specific heat C_{sg}. It gives an entropy of about R ln 2 at 45 K combined with the contribution from the second anomaly in C_S, which means that this contribution, in fact, can be related to the magnetic ordering in this material.

From the lattice part of the specific heat the Debye temperature is calculated by [44]

$$\theta_D = \left(\frac{12p\pi^4 R}{5B_3}\right)^{1/3}$$

with R the universal gas constant and p the number of atoms in each unit cell (see table 1). Using the B_3 from model III a value of $\theta_D = 335$ K is obtained. The value is in reasonable agreement with measurements on lattice specific heat in similar systems [41, 45].

4. Discussion

The investigated $Dy_{0.5}Sr_{0.5}MnO_3$ single crystal displays the basic properties of a spin-glass system, including a bifurcation in field-cooled and zero-field-cooled magnetization, dynamic critical slowing down and a small hysteresis in the isothermal magnetization at lower temperatures. The thermal magnetization data and electronic resistivity are rather similar to data reported earlier for polycrystalline $Dy_{0.5}Sr_{0.5}MnO_3$ [18, 19] and $Ho_{0.5}Sr_{0.5}MnO_3$. The large Dy moment masks the thermal magnetic response: therefore, the extraction of spin-glass properties for dynamical scaling analysis is difficult. The observed irreversibility in the thermal magnetization, the violation of H/T scaling of magnetization, the presence of a small hysteresis at low temperatures and, in particular, the analysis of the ac susceptibility are combined evidence that $Dy_{0.5}Sr_{0.5}MnO_3$ indeed shows a spin-glass state. The critical exponent $z\nu$ conforms with the values observed in canonical spin glasses, which are in the range of 2–12 [15]. The irreversibility in magnetization and slow dynamics is commonly attributed to classical spin-glass systems, but recent understanding is that such behavior signifies only a collective relaxation behavior. Because our fit of this critical slowing down is relatively insecure, this finding should not be taken

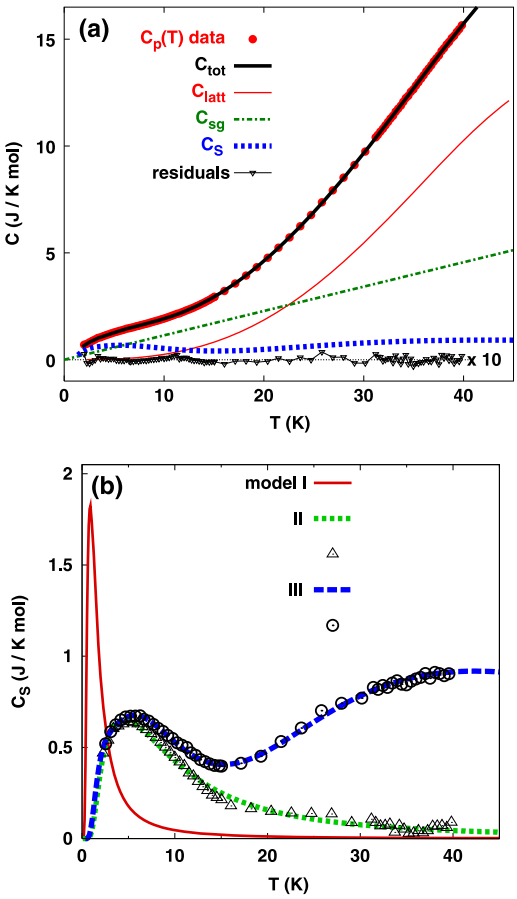

Figure 8. (a) Specific heat in the low temperature range. The total fitting curve C_{tot}, residuals and the different contributions shown are determined using equation (3*a*) with parameters for model III from table 1. (b) The Schottky-like contributions for the different models I, II and III as specified in table 1. Symbols show the extracted Schottky contribution as determined by the difference $C(T) - C_{latt} - C_{sg}$ for models II and III.

as proof of a homogeneous microscopic spin-glass state. In this regard, it is noteworthy that the characteristic microscopic time τ_0 for the relaxation in the $Dy_{0.5}Sr_{0.5}MnO_3$ system is large compared to other manganite spin-glass systems, where smaller values (10^{-10} s) are found [40]. This points towards the necessity of further detailed investigations such as, for example, an improved scaling analysis near the spin-glass temperature to conclude whether this manganite displays a true spin-glass state similar to canonical spin-glasses, or whether the complex magnetic properties are related to a phase-separated state [46]. In this connection, the investigation by Autret *et al* on $Ho_{0.5}Sr_{0.5}MnO_3$ [23] is interesting, as they find rather similar magnetic properties while also presenting evidence for a structural phase mixture even at room temperature with evidence for an A-type AFM order. Therefore, a clustered system of frustrated interacting magnetic entities may underlie our observation of spin-glass-like dynamics in $Dy_{0.5}Sr_{0.5}MnO_3$.

The resistivity versus temperature poses an interesting problem, as the best description is given by a variable-hopping model with an anomalous exponent. No transition into a conducting phase in large external fields could be observed: however, the overall magnetoresistance in the paramagnetic state is large and warrants an important contribution of spin scattering to the resistivity. Also, from our measurements no evidence for a charge order has been found for $Dy_{0.5}Sr_{0.5}MnO_3$, which is consistent with the phase diagrams presented for the Sr-doped 50:50 manganites (see, e.g., [8, 5]).

A high value of the specific heat is observed in these systems and a Schottky-like anomaly is seen at 5 K. As we have seen, a distribution of two-level Schottky functions is necessary to fit the specific-heat data in the low temperature range. This requires inhomogeneous local fields in these samples, which is consistent with a homogeneous spin-glass-like state. However, a nanoscale mixture from AFM and FM regions would also possibly yield a smeared Schottky-like anomaly related to the Zeeman-split 4f ground state of Dy^{3+}. The large low temperature specific heat in this material is related to large contributions from magnetic ordering. It has been found that a linear contribution C_{sg} is necessary, which is also consistent with a homogeneous dense spin-glass system.

5. Conclusions

The $Dy_{0.5}Sr_{0.5}MnO_3$ displays spin-glass-like properties, which are of interest, as they arise in a system where nanoscale electronic phase separation between different homogeneously magnetic phases, even with different structures, or a genuine homogeneous spin-glass phase may exist. The bifurcation observed in FC/ZFC cycles of dc magnetization and the anomalies in real and imaginary parts of ac susceptibility indicate a spin-glass-like phenomenon with a $T_g \approx 32$ K. The fact that these anomalies are centered around the same temperature suggests that they have the same origin. Further evidence for glassy magnetic properties has been obtained from a relatively large linear contribution to the low temperature specific heat, and from the smeared and wide Schottky anomaly related to inhomogeneous internal fields at Dy sites. The present data are overall consistent with a homogeneous spin-glass phase in $Dy_{0.5}Sr_{0.5}MnO_3$, but more detailed investigations, in particular detailed spin-glass scaling studies and microscopic probes on structural inhomogeneities at low temperatures, are necessary to ascertain this interpretation.

Acknowledgments

The authors acknowledge the financial support from the Department of Science and Technology, Government of India through the FIST program. One of us (HLB) also acknowledges the financial support from CSIR, India. SW thanks the European Commission for grant CoMePhS 517039.

References

[1] Mahesh R, Mahendiran R, Raychaudhuri A K and Rao C N R 1995 *J. Solid State Chem.* **120** 204
[2] Mahesh R and Itoh M 1999 *Phys. Rev.* B **60** 2994

[3] Miura N, Kerschl P, Kozlova N V, Nenkov K, Dörr K, Müller K-H, Kirste A, Hansel S, von Ortenberg M, Tokura Y, Akahoshi D and Tomioka Y 2006 *J. Phys.: Conf. Ser.* **51** 75–8
[4] Maignan A, Martin C, Van Tendeloo G, Hervieu M and Raveau B 1999 *Phys. Rev.* B **60** 15214
[5] Tokura Y 2006 *Rep. Prog. Phys.* **69** 797
[6] Rodriguez-Martinez L M and Attfield J P 1996 *Phys. Rev.* B **54** R15622
[7] Akahoshi D, Uchida M, Tomioka Y, Arima T, Matsui Y and Tokura Y 2003 *Phys. Rev. Lett.* **90** 177203
[8] Nakajima T, Yoshizawa H and Ueda Y 2004 *J. Phys. Soc. Japan* **73** 2283
[9] Sundaresan A, Maignan A and Raveau B 1997 *Phys. Rev.* B **56** 5092
[10] Wang K F, Wang Y, Wang L F, Dong S, Yu H, Li Q C, Liu J-M and Ren Z F 2006 *Appl. Phys. Lett.* **88** 152505
[11] Kuwahara H, Tomioka Y, Asamitsu A, Moritomo V and Tokura Y 1995 *Science* **270** 961
[12] Wang X L, Horvat J, Liu H K and Dou S X 1998 *J. Magn. Magn. Mater.* **182** L1–4
[13] Tomioka Y, Okimoto Y, Jung J H, Kumai R and Tokura Y 2003 *Phys. Rev.* B **68** 094417
[14] Arulraj A, Gundakaram R, Biswas A, Gayathri N, Raychaudhuri A K and Rao C N R 1998 *J. Phys.: Condens. Matter* **10** 4447
[15] Mydosh J A 1993 *Spin Glasses: An Experimental Introduction* (London: Taylor and Francis)
[16] Knížek K, Jirák Z, Pollert E, Zounová F and Vratislav S 1992 *J. Solid State Chem.* **100** 292
[17] García-Landa B, DeTeresa J M, Ibarra M R, Ritter C, Drost R and Lees M R 1998 *J. Appl. Phys.* **83** 7664
[18] Kasper N V, Troyanchuk I O, Chobot A N, Szymczak H and Fink-Finowicki J 1997 *J. Phys.: Condens. Matter* **9** 7455–61
[19] Terai T, Sasaki T, Kakeshita T, Fukuda T, Saburi T, Kitagawa H, Kindo K and Honda M 2000 *Phys. Rev.* B **61** 3488
[20] Chatterjee S and Nigam A K 2002 *Phys. Rev.* B **66** 104403
[21] Woodward P M, Vogt T, Cox D E, Arulraj A, Rao C N R, Karen P and Cheetham A K 1998 *Chem. Mater.* **10** 3652–65
[22] Woodward P M, Cox D E, Vogt T, Rao C N R and Cheetham A K 1999 *Chem. Mater.* **11** 3528–38
[23] Autret C, Martin C, Maignan A, Hervieu M, Raveau B, André G and Bourée F 2002 *J. Solid State Chem.* **165** 65–73
[24] Rietveld H M 1969 *J. Appl. Crystallogr.* **2** 65
[25] Rodriguez-Carvajal J 1993 *Physica* B **192** 55–69
[26] De Teresa J M, Ibarra M R, García J, Blasco J, Ritter C, Algarabel P A, Marquina C and del Moral A 1996 *Phys. Rev. Lett.* **76** 3392
[27] Bean C P and Jacobs I S 1956 *J. Appl. Phys.* **27** 1448
[28] Rao C N R, Arulraj A, Cheetham A K and Raveau B 2000 *J. Phys.: Condens. Matter* **12** R83–106
[29] Peña O, Bahout M, Gutierrez D, Duran P and Moure C 2003 *Solid State Sci.* **5** 1217
[30] Shklovskii B I and Efros A L 1984 *Electronic Properties of Doped Semiconductors* (Berlin: Springer)
[31] Mott N F 1993 *Conduction in Non-Crystalline Materials* (Oxford: Clarendon)
[32] Viret M, Ranno L and Coey J M D 1997 *Phys. Rev.* B **55** 8067
[33] Jaime M, Hardner H T, Salamon M B, Rubinstein M, Dorsey P and Emin D 1997 *Phys. Rev. Lett.* **78** 951
[34] Sheng L, Xing D Y, Sheng D N and Ting C S 1997 *Phys. Rev. Lett.* **79** 1710
[35] Emin D and Holstein T 1969 *Ann. Phys.* **53** 439
[36] Neifeld E A, Arkhipov V E, Ugryumova N A, Korolyov A V and Mukovsky Ya M 2007 *Low Temp. Phys.* **33** 264
[37] Haupt L, von Helmolt R, Sondermann U, Bärner K, Tang Y, Giessinger E R, Ladizinsky E and Braunstein R 1992 *Phys. Lett.* A **165** 473
[38] Wang K F, Wang Y, Wang L F, Dong S, Li D, Zhang Z D, Yu H, Li Q C and Liu J-M 2006 *Phys. Rev.* B **73** 134411
[39] Katzgraber H G, Körner M and Young A P 2006 *Phys. Rev.* B **73** 224432
[40] Nair S and Nigam A K 2007 *Phys. Rev.* B **75** 214415
[41] Hamilton J J, Keatley E L, Ju H L, Raychaudhuri A K, Smolyaninova V N and Greene R L 1996 *Phys. Rev.* B **54** 14926
[42] López J, de Lima O F, Lisboa-Filho P N and Araujo-Moreira F M 2002 *Phys. Rev.* B **66** 214402
[43] Ghosh N, Elizabeth S, Bhat H L, Rößler U K, Nenkov K, Rößler S, Dörr K and Müller K-H 2004 *Phys. Rev.* B **70** 184436
[44] Kittel C 1971 *Introduction to Solid State Physics* 4th edn (New York: Wiley)
[45] Lees M R, Petrenko O A, Balakrishnan G and McK Paul D 1996 *Phys. Rev.* B **59** 1298
[46] Rivadulla F, López-Quintela M A and Rivas J 2004 *Phys. Rev. Lett.* **93** 167206